VALIDATION OF OPERATIONAL GLOBAL WAVE PREDICTION MODELS WITH SPECTRAL BUOY DATA

K. M. Wingeart, T. H. C. Herbers, W. C. O'Reilly[1], P. A. Wittmann[2], R. E. Jensen[3], H. L. Tolman[4]

Abstract: Global wave predictions produced at two U. S. forecasting centers, Fleet Numerical Meteorology and Oceanography Center (FNMOC) and the National Centers for Environmental Prediction (NCEP) are evaluated with spectral buoy measurements. Previous validation studies of global wave models were based primarily on wave height data from operational satellite altimeters and moored in-situ buoys (e.g., Komen et al., 1994; Wittmann and Clancy, 1993). Fewer comparisons of frequency spectra and directional wave properties have been reported. In this study, data from directional wave buoys are used to examine the fidelity of frequency-directional spectra predicted by WAM and WAVEWATCH III (WW3) at the operational centers. The buoys used in the comparisons include 3-meter discus buoys operated by the National Data Buoy Center (NDBC) and Datawell waverider buoys deployed primarily along the California coast by the Scripps Institution of Oceanography Coastal Data Information Program (CDIP). Only buoys located in deep water are used in the comparisons. Here, preliminary results are presented for two locations, Point Conception, California and Christmas Island. Model nowcasts of frequency spectra and mean wave direction are compared to buoy measurements over a six-month period from 01 October 2000 to 31 March 2001. Individual swell events were identified in the spectra from the three models and the buoy data. Predicted and observed swell frequencies and arrival directions are compared, as well as the total energy transported past the buoy over the duration of each individual event.

[1] Department of Oceanography, Code OC/He, Naval Postgraduate School, Monterey, CA 93940, herbers@oc.nps.navy.mil

[2] Fleet Numerical Meteorology and Oceanography Center, 7 Grace Hopper Ave., Monterey, CA 93940

[3] U. S. Army Engineer Waterways Experiment Station, Coastal and Hydraulics Laboratory, Vicksburg, MS 39180

[4] SAIC-GSO at NOAA-NCEP, Ocean Modeling Branch, Environmental Modeling Center, 5200 Auth Road, Room 209, Camp Springs, MD 20746

Two separate implementations of the WW3 model generally outperformed WAM.

INTRODUCTION

Third generation wave prediction models that describe the evolution of the two-dimensional ocean wave spectrum are widely used in global and regional applications. The first of these models, WAM, was developed in 1988 by the WAMDI Group and was adopted for operational use by the Fleet Numerical Meteorology and Oceanography Center (FNMOC) in 1994. It solves the wave action balance equation in spherical coordinates for a two-dimensional wave spectrum. The global WAVEWATCH III (WW3) model, operational at the National Center for Environmental Prediction (NCEP), was first developed for shelf sea applications by Tolman (1991), and is gaining wide acceptance in the wave forecasting community. It is similar to WAM in structure, but incorporates wave-current interactions, a more sophisticated third-order numerical propagation scheme, and new formulations of wind input and dissipation source terms (Tolman and Chalikov, 1996). In 2001, WW3 replaced WAM at FNMOC as the operational wave prediction model.

In the present study, three global wave prediction models from FNMOC and NCEP are validated using spectral buoy information from the Coastal Data Information Program (CDIP) and the National Data Buoy Center (NDBC). The three models are WAM (implementation WAM, cycle 4.0, Wittmann and Clancy, 1993) and WW3 at FNMOC and WW3 at NCEP. Until recently, both WAM and WW3 were run in parallel at FNMOC, on a global 1° latitude by 1° longitude grid, with an integration domain extending from 78 N to 78 S. Both models have identical land mass and ice edges. The WAM model is forced by the Navy's atmospheric prediction system NOGAPS 3.4 surface wind stress, and WW3 at FNMOC is forced by NOGAPS 3.4 winds at 10 meter elevation. Both models use a three-hour wind time step. The WW3 model at NCEP uses a 1° latitude by 1.25° longitude grid and a dynamically adjusted ice edge updated daily from NCEP's automated passive microwave sea ice concentration analysis (Grumbine, 1996). The winds are adjusted to 10 meter elevation assuming neutral stability from NCEP's operational Global Data assimilation Scheme (GDAS) and the Aviation cycle of the Medium Range Forecast model (AVN). All three models use approximately the same spectral discretization with 25 frequencies that are logarithmically spaced with an increment factor of 1.1 and 24 directions that span 360° in 15° increments. The wave model time step in WAM is fixed for both the propagation and source terms (20 minutes). The WW3 model uses a variable time step for both propagation and source term integration to increase the model efficiency. The overall time step is one-hour, with a minimum of 5 minutes for the source term and a maximum of 1300 seconds for the propagation time step (Tolman, 1999). An important difference between the models is the more rapid wave growth under strong wind forcing in the WW3 models. Tolman and Chalikov (1996) show that the WW3 model is insensitive to numerical errors for wind speeds greater than 10 ms^{-1} due to the scaling behavior. The WW3 wind input source term becomes negative for wave that travel faster than the wind or at large angles to the wind, is 2-3 times smaller than WAM for fully developed seas, but larger at high frequencies.

The objective of this study was to test the WW3 model implementation at FNMOC and to develop a methodology for comparing spectral information from the models with buoy data. The study was conducted over a six-month period from 01 October 2000 to 31 March 2001, generally considered to be the Northern Hemisphere winter. Preliminary comparisons of the three models are presented at two deep water locations, near Point Conception (CDIP buoy in 597m depth), off the coast of southern California, and Christmas Island (NDBC buoy in 4755m depth) on the equator and south of Hawaii. The NDBC buoy at Christmas Island was a 3-meter discus buoy that also provided directional data. The buoys were used as ground truth in evaluating model predictions of swell energy as a function of frequency and time as well as the directional characteristics of the swells.

ANALYSIS

A simple methodology is presented for evaluating swell spectra predictions with spectral buoy data. All three models produce a nowcast (or analysis run) every 12 hours at 00Z and 12Z. The NDBC buoys record data every hour and the CDIP buoys record data every 30 minutes. Data from all buoys were averaged down to one record every three hours to provide smoother records for statistical analysis. Swell events were identified by tracking peaks in the wave frequency spectrum $E(f,t)$ in time. The frequencies, directions, arrival times, and bulk energy of swell events predicted by the models, are compared with the buoy measurements to assess the model performance.

Identifying Swell Events

The first step was to identify swell events in the energy spectrum as a function of frequency and time. Energy spectra are often bimodal, indicating the presence of swells arriving from different sources. Only swell events that were reasonably well separated in frequency were considered for comparison, using a simple criterion

$$\frac{|f_1 - f_2|}{|f_1 + f_2|} \geq 0.15 \qquad (1)$$

where f_1 and f_2 are adjacent peak frequencies in the frequency spectrum (see Figure 1).

Tracking Swell Events

The next step was to track swell events in time as well as frequency. Contour plots of wave energy as a function of frequency and time illustrate the evolution of swells from the early arrival at low frequencies to the decay at higher frequencies as time increases (see also Munk et al., 1963). The swell systems arrive at rapid intervals, usually causing the simultaneous presence of multiple swell events that show up as distinct peaks in the spectrum. After tracking the spectral peaks as a function of time, the swell events were terminated when peak frequencies changed by more than 20% over a 12 hour period. Since both the Point Conception and Christmas Island buoys had directional data available, a second criterion was applied. The event was terminated when the mean direction at the peak frequency changed by more than 30° in a 12 hour period. Events lasting less than 48 hours were discarded.

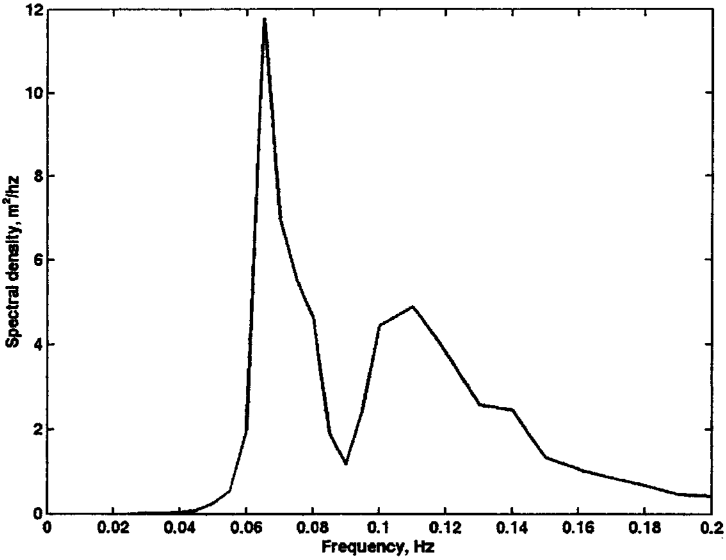

Fig. 1. Example of a bimodal energy spectrum indicating multiple swell arrivals

POINT CONCEPTION RESULTS

Figure 2 compares the swell evolution predicted by the three models with observations from the Point Conception buoy. Both WW3 models capture the swell arrivals very well. The WAM model, however, smoothes out the energy and blends two to three swell events into one event. Several possible reasons can explain this smoothing. WAM uses a first-order upwind propagation scheme and tends to diffuse swell energy as distance from the generation source increases. The WW3 models using a third order scheme, are expected to be less diffusive.

Other differences between WAM and WW3 that may contribute to the superior performance of WW3 in this case are the differences in the dissipation terms. The total dissipation source term for WW3 is defined as a linear combination of low-frequency and high-frequency terms (Tolman and Chalikov, 1996).

The predicted and observed swell peak frequencies and mean arrival directions (at the peak frequency) are compared in Figure 3. All three models fail to capture the early arrival of the waves at low frequencies and WAM does not track events into the higher frequencies. Generally, all three models capture frequency and mean direction of swell events very well. WAM mean directions are typically 5-10° further north than the buoy mean directions. During the periods when WAM smoothes multiple events together, the predicted directions do not correspond well with the buoy data. Figure 4 shows the energy flux,

$$\rho g \int E(f) C_g(f) df \tag{2}$$

neglecting directional spreading, versus time for one representative swell event. The energy flux was integrated over the frequency range $0.85 f_p$ to $1.15 f_p$, where f_p is the peak frequency, ρ is the density of sea water, g is gravity, $C_g(f)$ is the group speed, and $E(f)$ is the spectral energy. All models underestimated the energy flux for the event. The models also do not predict the early arrival of the swell event.

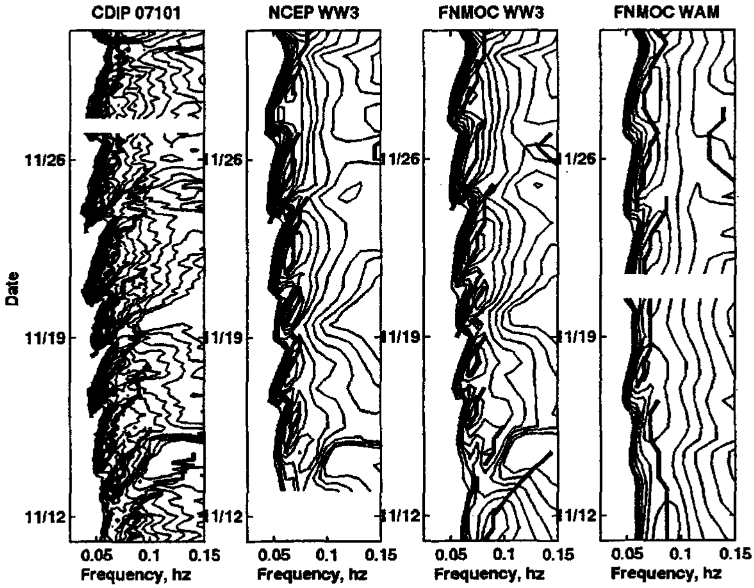

Fig. 2. Contours of spectral energy versus frequency and time for a twenty day period that is representative of the entire six-month study for the Point Conception site. Gaps in the contour lines indicate time periods for which no buoy observations or model predictions were available. Solid lines indicate events identified and tracked in time.

To compare swell events predicted by the models with those observed by the buoy, individual events were matched using the following criteria: (*i*) the model swell mean direction was within 30° of the buoy mean direction, (*ii*) model swell event start/end times were within 36 hours of buoy event start/finish time, and (*iii*) model peak frequency was within 20% of buoy peak frequency. Both WW3 models resolve more of the swell events that were measured by the Point Conception buoy than WAM. Of the 33 events detected by the buoy, 29 events were resolved by FNMOC WW3 and 24 events by NCEP WW3, whereas WAM resolved only 7 events.

The total wave energy transported past the buoy or model grid point (per unit crest length) over the duration of each individual swell event,

$$\rho g \iint C_g(f) E(f)\, df\, dt \tag{3}$$

was computed for all events in the six month study (Figure 5). All models under-predict the total energy for Point Conception. Both WW3 models have very similar results with lower bias and less scatter than WAM. As noted earlier, possible explanations for these differences include the first-order upwind propagation scheme in WAM diffusing energy, a better representation of rapid wave growth under strong wind forcing in the WW3 models, and differences in the wind input and dissipation source terms.

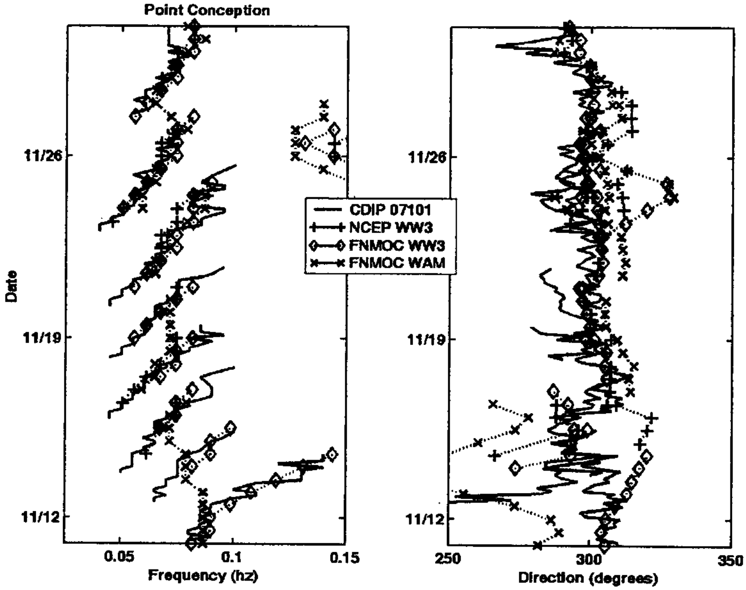

Fig. 3. Point Conception swell comparisons. Predicted and observed peak frequencies versus time are shown in the left panel. Corresponding mean directions are shown in the right panel.

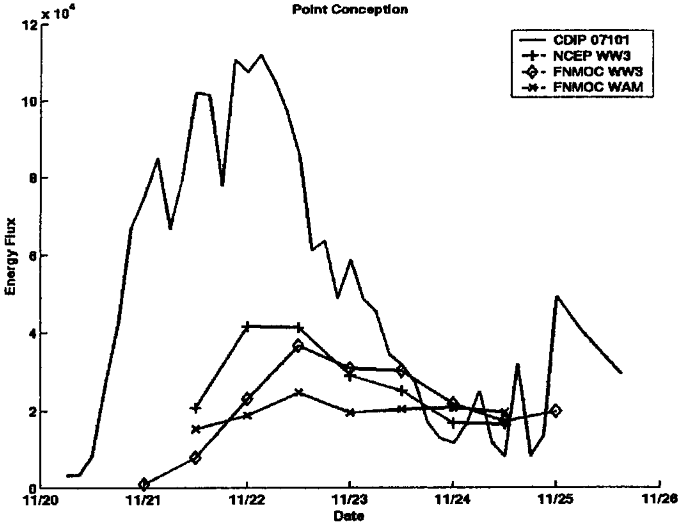

Fig. 4. Energy flux in W/m for one swell event at the Point Conception site. All three models underestimate the energy flux and do not predict the early arrival of the event measured by the buoy.

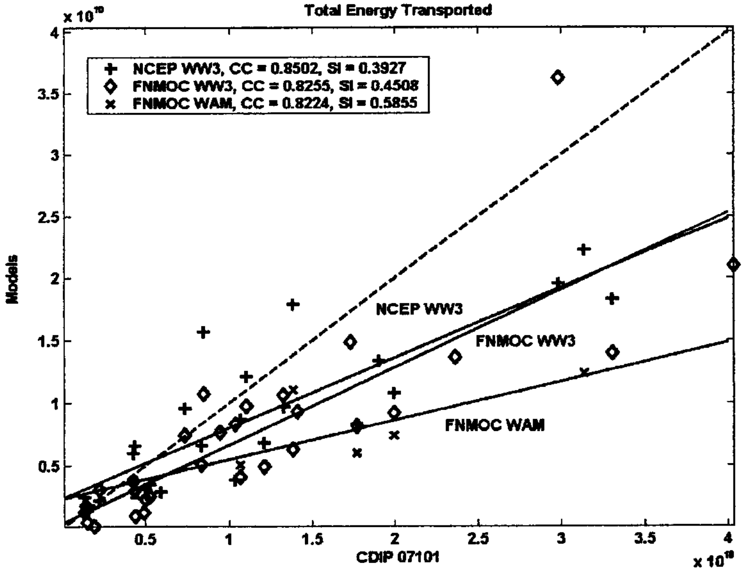

Fig. 5. Scatter plot of total predicted versus observed energy in J/m transported through the Point Conception site (per unit crest length). Each symbol represents one swell event captured by both the model and the buoy. The solid lines are the

best fit lines, the dashed line is the one to one correspondence line. In the legend, CC is the correlation coefficient and SI is the scatter index for the model.

CHRISTMAS ISLAND RESULTS

Figure 6 shows contours of swell energy versus frequency and time for a representative twenty day period at the Christmas Island site. All three models capture the spectral evolution well, with the exception of frequencies greater than 0.1 Hz that were dominated by energetic seas generated by the strong easterly winds that prevail for the Northern Hemisphere winter along the equator. This easterly wind produced a continual fully developed sea with peak frequency of about 0.1 to 0.17 Hz. All models grossly under-predict the energy levels of these seas. For example, notice the swell event predicted by all three models on 03 December not detected in the buoy data. The contours indicate that the buoy is picking up some energy in the low frequencies, but a more energetic high frequency peak from the equatorial winds masks this low frequency peak. At lower frequencies, the observed and predicted wave field was dominated by northwesterly swell. Often the swell energy levels are much lower than those of the equatorial easterly wind seas, and as a result, the analysis is less successful in identifying swell events.

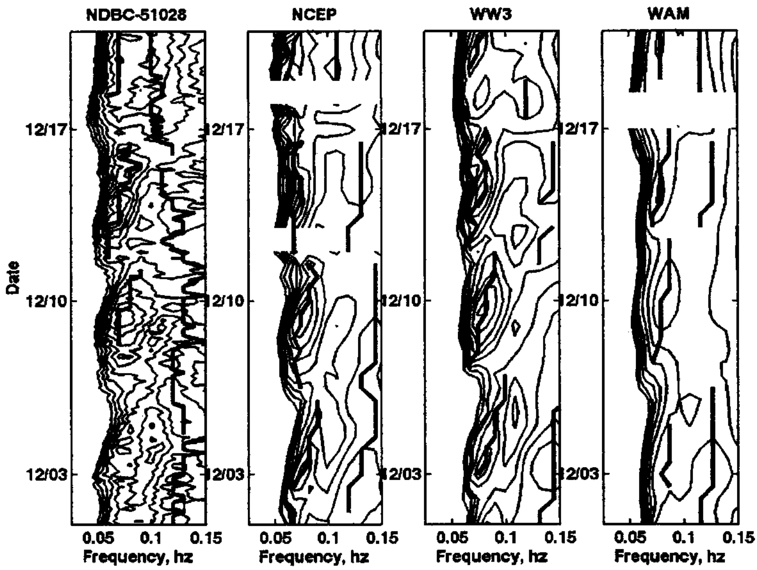

Fig. 6. Contours of spectral energy versus frequency and time for a twenty day period that is representative of the entire six-month study for the Christmas Island site. Gaps in the contour lines indicate time periods for which no buoy observations or model predictions were available.

Of the 22 swell events detected in the Christmas Island buoy measurements, 15 were resolved by FNMOC WW3 and 16 by NCEP WW3. WAM performed better at this site than at Point Conception, resolving 13 events. Although there is considerable scatter in the energy comparisons (Figure 7), FNMOC WW3 appears to do better in this location than NCEP WW3. The large difference between the FNMOC WW3 and the NCEP WW3 can only be explained by the difference in the atmospheric forcing. Generally, in the North Pacific, both AVN and NOGAPS have similar wind fields, but along the equator, small differences in the wind fields can lead to large differences in the swell predictions. Atmospheric data in the southern hemisphere is generally more sparse than in the northern hemisphere, so the NOGAPS wind field can be distinctly different from the AVN wind field in this region, which would impact swell generation.

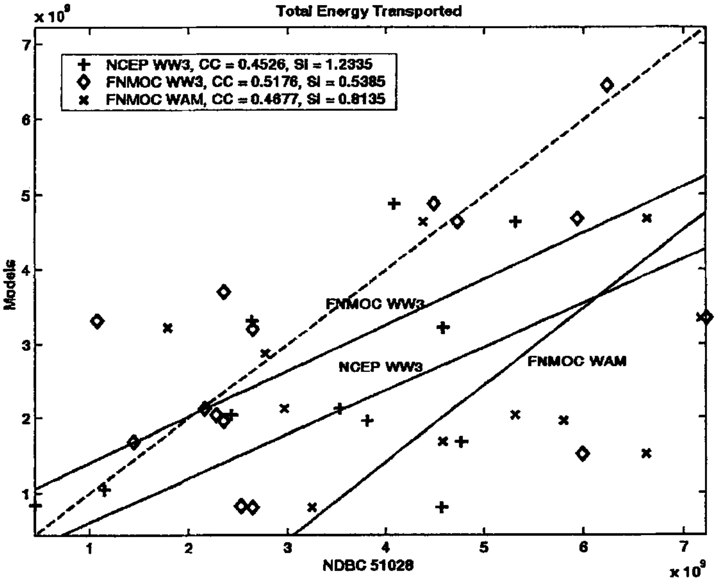

Fig. 7. Scatter plot of total predicted versus observed energy in J/m transported through the Christmas Island site (per unit crest length). Each symbol represents one swell event captured by both the model and the buoy. The solid lines are the best fit lines, the dashed line is the one to one correspondence line. In the legend, CC is the correlation coefficient and SI is the scatter index for the model.

CONCLUSIONS

The purpose of this study is to develop a methodology for comparing spectral information from global wave prediction models with buoy data. Swell events were identified by tracking well separated peaks in the E(*f*) spectrum in time. Preliminary results for a site near Point Conception indicate that all three models under-predicted the total energy for a swell event. The WW3 predictions resolved swell events better than the WAM predictions, and yielded more accurate energy estimates. Comparisons near Christmas Island were more complicated owing to energetic seas from the continuous equatorial easterly winds present in the Northern Hemisphere winter that tend to overwhelm the low frequency swells. Consequently, fewer swell events could be resolved and the energy comparisons show more scatter. These results are preliminary, further comparisons will be conducted at 13 additional CDIP and NDBC buoy locations.

REFERENCES

Grumbine, R.W., 1996. Automated passive microwave sea ice concentration analysis at NCEP. NWS/NCEP/OMB Technical Note 120, 13 pp.

Komen, G., Cavaleri, L., Donelan, M., Hasselmann, K., Hasselmann, S., and Janssen, P. 1994. Dynamics and Modeling of Ocean Waves. Cambridge University Press, 532 pp.

Munk, W. H., Miller, G. R., Snodgrass, R. E., and Barber, N. F. 1963. Directional Recording of Swell from Distant Storms. Institute of Geophysics and Planetary Physics, 255, 506-584.

Tolman, H. L. 1991. A third-generation model for wind waves on slowly varying, unstead, and inhomogeneous depths and currents. *Journal of Physical Oceanography*, 21, 782-797.

Tolman, H. L. 1992. Effects of numerics on the physics in a third-generation wind-wave model. *Journal of Physical Oceanography*, 22(10), 1095-1110.

Tolman, H. L. and Chalikov, D. 1996. Source terms in a third-generation wind-wave model. *Journal of Physical Oceanography*, 26, 2497-2518.

Tolman, H. L. 1999a. User manual and system documentation of WAVEWATCH-III version 1.18. NOAA/NWS/NCEP/OMB Technical Note 166, 110 pp.

The WAMDI Group. 1988. The WAM Model: A third-generation ocean wave prediction model. *Journal of Physical Oceanography*, 18, 1775-1810.

Wittmann, P. A. and Clancy, R. M. 1993. Implementation and validation of a global third-generation wave model at Fleet Numerical Oceanography Center., *Proceedings of the Second International Symposium Ocean Wave Measurement and Analysis* , 406-419.